Eur. Phys. J. B **44**, 481–486 (2005)
DOI: 10.1140/epjb/e2005-00147-x

THE EUROPEAN PHYSICAL JOURNAL B

Optical nonlinearity enhancement of compositionally graded films

Lei Gao [a]

Department of Physics, Suzhou University, Suzhou 215006, China

Received 25 December 2004
Published online 30 May 2005 –

Abstract. We present a theoretical description for the effective linear and nonlinear optical properties of compositionally graded films consisting of nonlinear metal particles and linear dielectric particles. The volume fraction of metal particles varies along the direction perpendicular to the film. To account for the composition gradient, we resort to effective medium approximation to investigate the equivalent (local) dielectric constant and third-order nonlinear susceptibility. As a result, the effective second-rank dielectric constant tensor and fourth-rank nonlinear optical susceptibility tensor are directly determined by regarding the graded film as a multilayer one. We predict that for a power-law composition gradient $p(z) = z^m$, the increase of m leads to large enhancement of the optical nonlinearity and hence the figure of merit in the high-frequency region. On the other hand, for a given total volume fraction, we find that the optical nonlinearity enhancement for the composition gradient case is larger than the one in non-graded case. Moreover, we can choose different graded profile to realize the appreciable optical nonlinearity enhancement. Therefore, the compositionally graded film can be served as a suitable candidate material for obtaining the large optical nonlinearity and optimal figure of merit.

PACS. 42.65.-k Nonlinear optics – 42.79.Ry Gradient-index (GRIN) devices – 72.20.Ht High-field and nonlinear effects – 77.84.Lf Composite materials

1 Introduction

There are practical needs for nonlinear optical composite materials that possess large nonlinear susceptibility coupled with a fast response time [1–4]. For instance, this kind of materials may be useful for the design of nonlinear optical devices, like ultrafast optical switches, and so on. By taking into account the local-field effect and the percolation effect, large optical nonlinearity has been found in multi-layer structures [5], in uniaxial anisotropic composites [6], and in metal/dielectric composites with shape distribution [7].

Recently, graded materials have attracted much interest in various engineering applications [8] due to their different physical properties from the homogeneous ones. In nature, there exist many graded materials, such as biological cells [9] and liquid crystal droplets [10]. To investigate the effective nonlinear optical properties of graded composites in which nonlinear spherical inclusions are randomly embedded in a host medium, we proposed a nonlinear differential effective dipole approximation (NDEDA) [11]. We showed an excellent agreement between the NDEDA and the first-principles approach [11]. To one's interest, the dielectric gradation in the nonlinear metal particles is found to be helpful to enhance both the optical nonlinear susceptibility and the figure of merit. Later, the idea was generalized to the dielectric graded films [12]. To the best of our knowledge, in above works, the gradation mainly results from the radial inhomogeneity of the local physical parameters such as the dielectric constant (or the electric conductivity).

On the other hand, spatially graded composites (SGC) are a new generation of engineered materials in which the geometric parameters such as the composition or microstructure morphology (rather than the local physical parameter) are gradually varied in one or more dimensions [13,14]. In contrast to traditional composite materials and graded composites with radial inhomogeneity, SGC possess many novel features, and hence have many realistic applications as electronic devices, optical films, and thermal barrier coatings. For example, metal-ceramic SGC are super-heat-resistant materials for aerospace applications. Generally, in SGC, the composition gradient is introduced to provide the mechanical coupling between the components. However, it will influence the effective properties of the SGC. In this connection, the effective thermal conductivity of the composite film with composition gradient has been investigated in references [15,16].

[a] e-mail: lgaophys@pub.sz.jsinfo.net

In this paper, we would like to study the effective linear and nonlinear optical properties of spatially graded metal-dielectric films. For such SGC, the volume fraction of the metal particles is assumed to vary along the direction perpendicular to the film. Thus, our present study are valid for all possible values of volume fractions of the metal particles. Moreover, the graded film possesses anisotropic linear and nonlinear optical properties, rather than isotropic physical properties in reference [7]. We will show that the presence of composition gradient plays a crucial role in enhancing the third-order nonlinear susceptibility as well as the figure of merit.

The paper is organized as follows. In Section 2, we present our theoretical development. In Section 3, numerical results are shown for the linear absorption and the optical nonlinearity enhancement, as well as the figure of merit, for various composition gradients. This paper ends with a discussion and conclusion in Section 4.

2 Theoretical development

Let us consider metallic/dielectric functionally graded film with width L along z-axis (see Fig. 1). In each z-slice, there are two components: one is the nonlinear metal with linear dielectric constant $\epsilon_1(\omega)$ and the third-order nonlinear susceptibility $\chi_1(\omega)$; the other is the linear dielectrics with dielectric constant ϵ_2. We assume the volume fraction of the nonlinear metal component to be $p(z)$ at the position z, which varies only in the z direction. Such a property is typical for a FGC. Moreover, we take the two faces of the film to lie at $z = 0$ and $z = L$.

To investigate the effective linear and nonlinear optical responses of the graded film, we must first obtain the equivalent (local) linear dielectric constant $\bar{\epsilon}(z,\omega)$ and nonlinear optical susceptibility $\bar{\chi}(z,\omega)$ for the z-slice, which are a function of the volume fraction at z. For the equivalent linear dielectric constant $\bar{\epsilon}(z,\omega)$, we resort to three-dimensional effective medium approximation, which receives the form [17]

$$p(z)\frac{\epsilon_1(\omega)-\bar{\epsilon}(z,\omega)}{\epsilon_1(\omega)+2\bar{\epsilon}(z,\omega)}+[1-p(z)]\frac{\epsilon_2-\bar{\epsilon}(z,\omega)}{\epsilon_2+2\bar{\epsilon}(z,\omega)}=0. \quad (1)$$

Equation (1) is applicable when two components percolate together over a composition range.

Consequently, we adopt the mean-field approximation to obtain the equivalent third-order nonlinear optical susceptibility $\bar{\chi}(z,\omega)$ [18,19],

$$\bar{\chi}(z,\omega)=\frac{\chi_1}{p(z)}\int_0^1\left(\frac{s(z,\omega)}{s(z,\omega)-x}\right)^2 \times m(x)\mathrm{d}x\cdot\int_0^1\left|\frac{s(z,\omega)}{s(z,\omega)-x}\right|^2 m(x)\mathrm{d}x, \quad (2)$$

where $s(z,\omega)\equiv\epsilon_2/[\epsilon_2-\epsilon_1(z,\omega)]$, and $m(x)$ is the spectral density function, which was well studied independently by Bergman [20] and Milton [21]. For three-dimensional

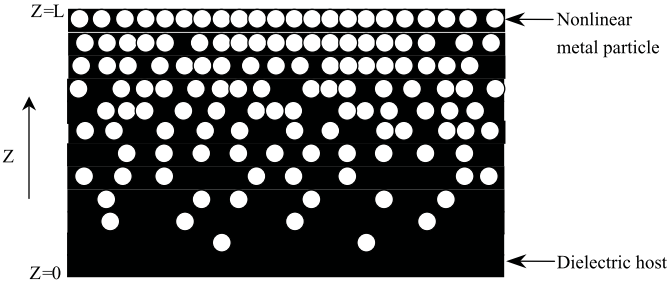

Fig. 1. A composite film with composition gradient.

effective medium approximation, $m(x)$ admits

$$m(x)=\frac{3p(z)-1}{2}\theta\left[3p(z)-1\right]\delta(x) + \begin{cases}\frac{3\sqrt{(x-x_1)(x_2-x)}}{4\pi x} & \text{if} \quad x_1<x<x_2\\ 0 & \text{otherwise,}\end{cases} \quad (3)$$

where $\theta(\cdots)$ is the step function and $x_{1,2}=\{1+p(z)\mp 2\sqrt{2p(z)[1-p(z)]}\}/3$.

Next, we aim at studying the effective linear dielectric constant tensor $\overleftrightarrow{\epsilon}_e$ and effective third-order nonlinear susceptibility tensor $\overleftrightarrow{\chi}_e$. Once $\bar{\epsilon}(z,\omega)$ and $\bar{\chi}(z,\omega)$ are known, the problem reduces to the one of multilayers [5]. For our simple geometry, the non-diagonal components of the second-rank tensor $\overleftrightarrow{\epsilon}_e$ are zero, while the diagonal components are given by

$$\frac{1}{\epsilon^e_{zz}}=\frac{1}{L}\int_0^L\frac{\mathrm{d}z}{\bar{\epsilon}(z,\omega)}, \quad (4)$$

if the electric field is polarized along z-axis, and

$$\epsilon^e_{xx}=\epsilon^e_{yy}=\frac{1}{L}\int_0^L\bar{\epsilon}(z,\omega)\mathrm{d}z, \quad (5)$$

if the electric field is polarized in the plane of the layers (i.e., $\mathbf{E}\perp\mathbf{z}$).

In general, the components of the effective third-order nonlinear optical susceptibility tensor $\overleftrightarrow{\chi}_e$ can be defined as follows,

$$\chi^e_{ijkl}E_{0,i}E_{0,j}E_{0,k}E^*_{0,l}= \frac{1}{L}\int_0^L\mathrm{d}z\bar{\chi}_{ijkl}(z,\omega)E_i(z,\omega)E_j(z,\omega)E_k(z,\omega)E^*_l(z,\omega), \quad (6)$$

where $\bar{\chi}_{ijkl}(z,\omega)$ is the components of the equivalent third-order nonlinearity, while $E_i(z,\omega)$ is the local field at position z, and has the form

$$E_i(z,\omega)=\begin{cases}\frac{\epsilon^e_{zz}}{\bar{\epsilon}(z,\omega)}E_{0,z} & \text{if} \quad i=z\\ E_{0,i} & \text{if} \quad i=x,y,\end{cases} \quad (7)$$

where $E_{0,i}$ is the applied field amplitude along i-axis.

Using equations (4), (5), and (6), the non-vanishing components of the four-rank tensor $\overleftrightarrow{\chi_e}$ can be written as,

$$\chi^e_{zzzz} = \frac{1}{L}\int_0^L \mathrm{d}z\bar{\chi}(z,\omega)\left|\frac{\epsilon^e_{zz}}{\epsilon(z,\omega)}\right|^2\left(\frac{\epsilon^e_{zz}}{\epsilon(z,\omega)}\right)^2,$$
$$\chi^e_{xxxx} = \chi^e_{yyyy} = \frac{1}{L}\int_0^L \mathrm{d}z\bar{\chi}(z,\omega),$$
$$\chi^e_{xxzz} = \chi_{zxxz} = \cdots = \frac{1}{3L}\int_0^L \mathrm{d}z\bar{\chi}(z,\omega)\left|\frac{\epsilon^e_{zz}}{\epsilon(z,\omega)}\right|^2,$$
$$\chi^e_{xzzx} = \chi^e_{zxzx} = \cdots = \frac{1}{3L}\int_0^L \mathrm{d}z\bar{\chi}(z,\omega)\left(\frac{\epsilon^e_{zz}}{\epsilon(z,\omega)}\right)^2. \quad (8)$$

In deriving equation (8), we have assumed that the local nonlinear susceptibility at the position z is electronic in nature, which implies that [22]

$$\bar{\chi}_{xxxx} = \bar{\chi}_{yyyy} = \bar{\chi}_{zzzz} = \bar{\chi}(z,\omega),$$
$$\bar{\chi}_{xyyx} = \bar{\chi}_{xyxy} = \bar{\chi}_{xxyy} = \cdots\frac{1}{3}\bar{\chi}_{xxxx}.$$

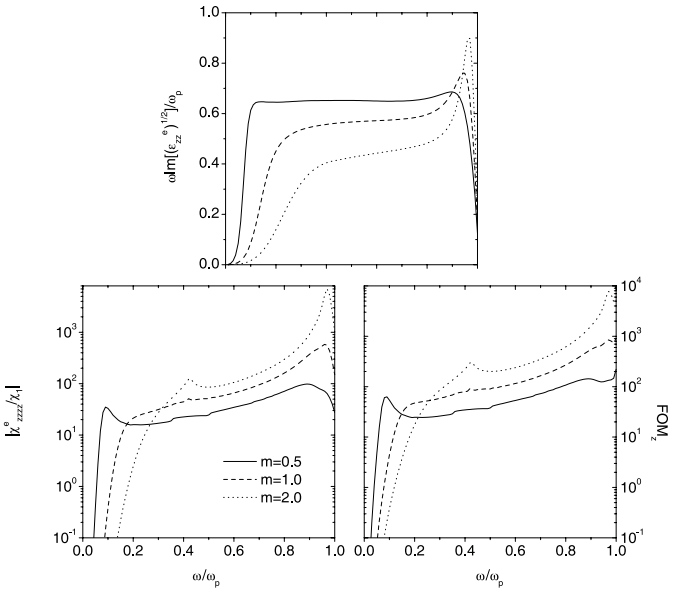

Fig. 2. The linear optical absorption $\omega\mathrm{Im}[\sqrt{\epsilon^e_{zz}}]/\omega_p$, optical nonlinearity $|\chi^e_{zzzz}/\chi_1|$, and FOM_z versus the normalized incident angular frequency ω/ω_p, for power-law composition gradient $p(z) = z^m$ with various m.

3 Numerical results

In what follows, we shall do some numerical calculations based on equations (4), (5) and (8). As a model system, we consider spherical particles to be a Drude-like metal, which has a linear dielectric constant of the form

$$\epsilon(r,\omega) = 1 - \frac{\omega_p^2}{\omega(\omega + \mathrm{i}\gamma)}, \quad (9)$$

where γ is the relaxation rate, and ω_p represents the plasma-frequency. For numerical calculations, we make additional assumption that the dielectric constituent has a frequency-independent dielectric constant $\epsilon_2 = (3/2)^2$ (static dielectric constant of water). Furthermore, to highlight the composite effect, a frequency-independent real value of $\chi_1(\omega)$ ($\equiv \chi_1$) is set.

Figure 2 displays the linear optical absorption coefficient $\alpha_{zz} \sim \omega/\omega_p\mathrm{Im}[\sqrt{\epsilon^e_{zz}}]$, optical nonlinearity enhancement $|\chi^e_{zzzz}/\chi_1|$ and figure of merit [$\mathrm{FOM}_z \equiv |\chi^e_{zzzz}|/(\chi_1\alpha_{zz})$] versus the normalized frequency ω/ω_p for a power-law profile in the volume fraction $p(z) = z^m$. As is evident from the results, there exists a broad band due to surface plasmon resonance in the range $0 < \omega < \omega_p$ for $m = 0.5$. As m increases, the center for the resonant band exhibits a blue-shift. At the same time, with increasing m, the volume fraction of metal particles becomes small, leading to narrow bands accompanied with small magnitude especially in the region $0 < \omega < 0.8\omega_p$. Moreover, for small z, as $p(z) = z^m$ will be smaller than 1/3 (the percolation threshold of metal component at each slice), the z slice is not metallic. Consequently, the graded film will be always insulating in the direction parallel to the z-axis, manifested by the absence of a Drude peak around zero frequency. For $|\chi^e_{zzzz}/\chi_1|$, we predict large enhancement of optical nonlinearity in the high-frequency region. To one's interest, such an enhancement becomes more prominent with increasing m. We can easily understand this as follows: with increasing m (or decreasing the volume fraction), much more isolated metallic clusters appear in the position z, which is helpful to enhance the surface plasmon resonance and enlarge the local field. As a result, the effective optical nonlinearity can be largely enhanced. The figure of merit (FOM) takes on the similar behavior as $|\chi^e_{zzzz}|/\chi_1|$. Interestingly, the FOM in the region $0.4\omega_p < \omega < \omega_p$ is quite useful for practical applications due to the fact that, in that region, the optical nonlinearity is enhanced, while the optical absorption is depressed. Therefore, the compositionally gradation is very useful to make the FOM attractive.

Similar considerations apply to the x (or y)-component. In Figure 3, we plot $\alpha_{xx} \sim \omega/\omega_p\mathrm{Im}[\sqrt{\epsilon^e_{zz}}]$, $|\chi^e_{zzzz}/\chi_1|$, and FOM_x against ω for $p(z) = z^m$ with various m. The optical absorption for the electric field polarized in the plane of the layers decreases monotonically with increasing ω, in contrast to the one shown in Figure 1. In this case, the equivalent electric field is spatially uniform, thus the effective dielectric constant becomes simple averages of the equivalent dielectric constant at z-slice. In this connection, the metallic behavior at large z-slice will lead to the metallic behavior of the graded film along x (or y)-axis. Therefore, a Drude peak appears, characterized by a fast increase of linear absorption at $\omega \sim 0$. The behavior of the optical nonlinearity enhancement is also quite different from the z-component in that it is determined by the geometric average of the equivalent nonlinear susceptibility (for the z component, it results from not only the contribution form the equivalent nonlinear susceptibility, but also the local field effect due to the compositional gradations). The above reason

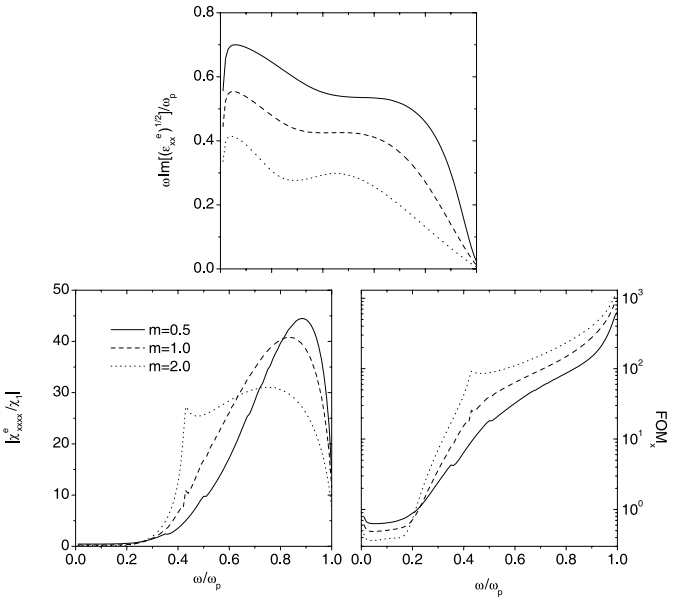

Fig. 3. Same as Figure 1, but for the x-component.

also accounts for the larger magnitude of the effective nonlinearity for z-component than the one for x-component. From the figure, we also note that the optical nonlinearity peak located at the high-frequency region is separated from the linear absorption one at the low-frequency one especially for small m, resulting in the appreciable FOM near $\omega \approx \omega_p$. Here, we would like to mention that the separation of two peaks has been predicted for a uniaxial anisotropic composite of metal nanocrystal in a dielectric host [6]. In addition, we find that by the adjustment of compositional gradation parameter m, we can obtain the large enhancement of FOM in the high-frequency region.

We also plot the optical nonlinearity enhancement for non-diagonal components in Figure 4. Again, large optical nonlinearity enhancement occurs at large ω especially for larger m.

Next, we would like to discuss the results of compositionally graded films with different profiles in the volume fraction $p(z)$, but containing the same total volume fractions of metal particles. We show the results for z-component in Figure 5 for two profiles $p(z) = z/L$ and $3(z/L)^{1/2}/4$. The non-gradient profile $p(z) = 1/2$ is also plotted for comparison. It is quite easy to demonstrate that the choices really satisfy the requirements:

$$\int_0^L \mathrm{d}z \frac{z}{L} = \int_0^L \mathrm{d}z \frac{3}{4}\sqrt{\frac{z}{L}} = \int_0^L \mathrm{d}z \frac{1}{2} = \frac{L}{2}. \qquad (10)$$

Although the volume fraction profile $p(z) = (3/4)\sqrt{z/L}$ has the same amount of metal particles as in the linear profile $p(z) = z/L$, the distribution of metal particles for a $\sqrt{z}$ profile leads to $p = 3/4$ at $z = L$, rather than $p = 1$ for a z profile. From Figure 5, we find that the results for different profiles are quite different, although the total volume fractions are the same. Both effective optical nonlinearity and FOM for linear profile are found to be enhanced in the frequency region $0.2 < \omega < 0.9\omega_p$, in

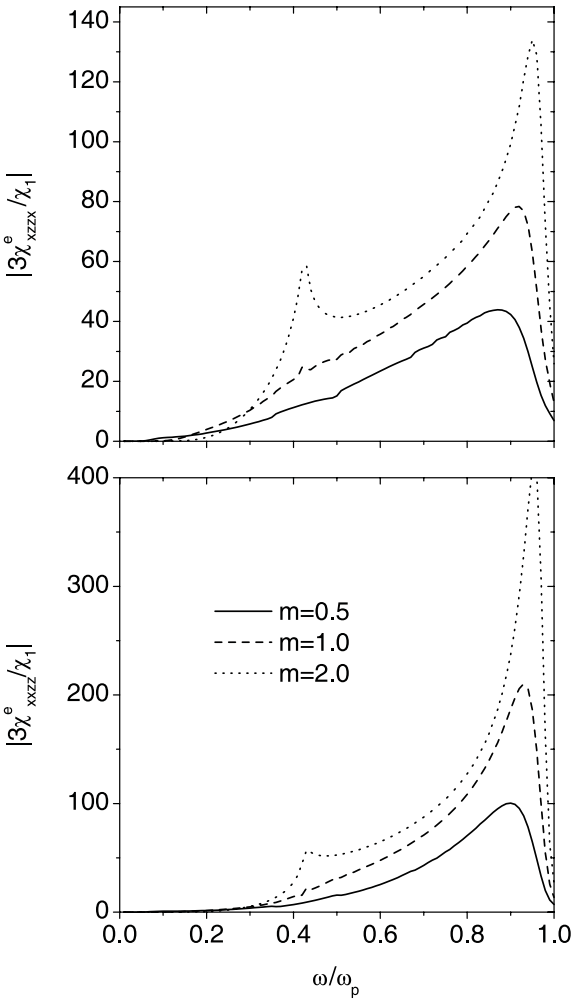

Fig. 4. The non-diagonal components of effective optical nonlinearity tensor as a function of ω/ω_p.

comparison with those for the $\sqrt{z}$ profile. The difference mainly results from the fact that there exists a broader z-region for linear profile than $\sqrt{z}$ profile, in which the volume fraction of metal particles is small. On the other hand, near ω_p, the FOM for $p(z) = (3/4)\sqrt{z/L}$ is one order magnitude larger than the one for linear profile. Furthermore, in the middle-frequency region $0.2 < \omega < 0.9\omega_p$, both the effective optical nonlinearity and FOM for composition gradient are larger than those for non-gradient case. Therefore, for a given total volume fraction, we can choose a suitable compositional gradation profile for the functionally graded film to realize the large enhancement of optical nonlinearity and further FOM.

4 Discussion and conclusion

In this paper, we investigate the effective linear and nonlinear optical properties of compositionally graded film in which the metal particles have weak nonlinearity. We give a detail description of the nonzero components of

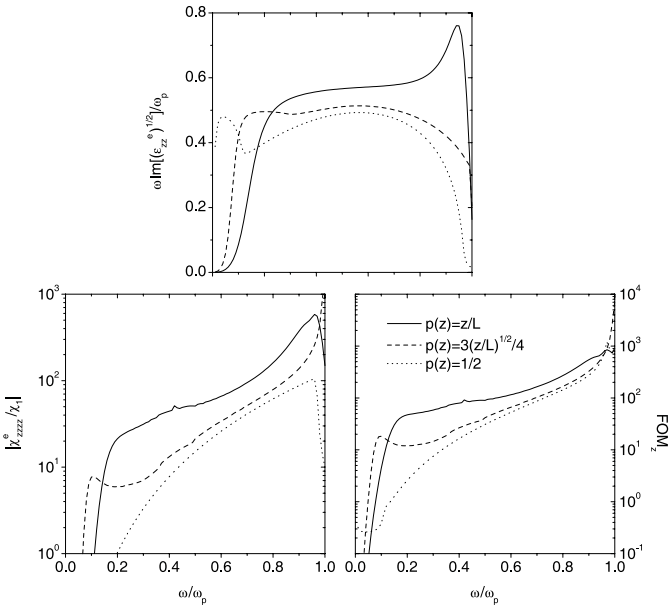

Fig. 5. Same as Figure 1, but for some composition gradients with the same total volume fractions.

the second-rank effective dielectric constant tensor and the fourth-rank effective nonlinear susceptibility tensor. The effect of the gradation profile on these nonzero components is studied. We found that for the power-law profile in the volume fraction $p(z) = z^m$, with increasing m, we can realize large optical nonlinearity enhancement and optimal FOM in the high-frequency region when the electric field is polarized along z-axis. On the other hand, if the electric field is polarized perpendicular z-axis, the adjustment of m is helpful to realize the separation of the optical nonlinearity peak from the absorption one, resulting in large figure of merit. For the same volume fraction of metal particles, we can choose different compositional profile to achieve large optical nonlinearity and FOM.

In our work, the theory was developed based on the assumption that the metallic particles are nonlinear, but the dielectric grains are linear. Actually, the work can be easily generalized to the case when both particles are nonlinear. In this instance, the equivalent (local) third-order nonlinear optical susceptibility $\bar{\chi}(z,\omega)$ should be written as,

$$\bar{\chi}(z,\omega) = \frac{\chi_1}{p(z)} \int_0^1 \left[\frac{s(z,\omega)}{s(z,\omega)-x}\right]^2 m(x)\mathrm{d}x \times \int_0^1 \left|\frac{s(z,\omega)}{s(z,\omega)-x}\right|^2 m(x)\mathrm{d}x + \frac{\chi_2}{1-p(z)} \times \left[1 - \int \frac{[|s(z,\omega)|^2 - x]m(x)}{|s(z,\omega)-x|^2}\mathrm{d}x\right] \times \left\{1 - \int \frac{\left[s^2(z,\omega)-x\right]m(x)}{[s(z,\omega)-x]^2}\mathrm{d}x\right\}, \quad (11)$$

where χ_2 is the nonlinear susceptibility of the dielectric particles.

In previous publications [6,23], by using the manipulation of anisotropic microstructure, one can separate the absorption peak from the nonlinearity enhancement peak in a suspension of metal nanocrystals in a dielectric host. In this paper, we have provided an alternative way, i.e., the use of compositional gradation, to achieve a large enhancement of third-order nonlinearity in a graded film. We note that the compositionally graded film also possesses an anisotropic optical nonlinear response, but we obtain a larger enhancement of optical nonlinearity than in references [6,23]. On the other hand, we would like to mention reference [24], in which the Maxwell-Garnett approximation was used to calculate the equivalent effective linear dielectric constant, and thus the calculation was restricted to the volume fraction much less than unity. For present study, we adopt effective medium approximation, which is valid for all possible values of volume fractions of metal particles. In this regard, the compositional gradation form can be chosen easily. Another difference is that the equivalent third-order nonlinear susceptibility in z-slice was assumed to be the same as that of the metal component in reference [24]. As the dielectric contrast $\epsilon_1(z,\omega)/\epsilon_2$ is large during calculations, such an assumption becomes rather rough. The optimal treatment should be adopted to obtain the equivalent (local) nonlinear susceptibility for z-slice, as done in our present work.

The nonlinearity under the present consideration is cubic. Consequently, the local fields inside the composite system take on the same frequency as the applied field, and harmonic generations are not included. However, for quadratic nonlinearity, the explicit dependence of the local dielectric response on the electric field vector will give rise to harmonic local fields in composites. In this regard, Levy et al. [25] have carried out the second and third harmonic generations in some inhomogeneous media, e.g., parallel slabs, dilute spherical inclusions, and so on. It would be of great interest to investigate the harmonic generations in compositionally graded composites.

Our theoretical investigations should be compared with experimental reports. As a matter of fact, the optical nonlinearity enhancement of both the parallel and perpendicular polarizations are related to the nonlinear phase shift, which can be measured by using Z-scan method [5]. Furthermore, the numerical simulations are now being carried out to check our predictions.

This work was supported by the National Natural Science Foundation of China under Grant No. 10204017 (L.G.) and the Natural Science of Jiangsu Province under Grant No. BK2002038 (L.G.).

References

1. D.J. Bergman, D. Stroud, *Solid State Physics: Advances in Research and Applications*, edited by H. Ehrenreich, D. Turnbull (Academic Press, New York, 1992), Vol. 46, p. 147
2. A.K. Sarychev, V.M. Shalaev, Phys. Rep. **335**, 275 (2000), and references therein

3. V.M. Shalaev, *Nonlinear Optics of Random Media: Fractal Composites and Metal-Dielectric Films* (Springer-Verlag, Berlin, 2000)
4. See, for example, the articles in *Proceedings of the Sixth International Conference on Electrical Transport and Optical Properties of Inhomogeneous Media*, Physica B **338**, (2003)
5. G.L. Fischer, R.W. Boyd, R.J. Gehr, S.A. Jenekhe, J.A. Osaheni, J.E. Sipe, L.A. Weller-Brophy, Phys. Rev. Lett. **74**, 1871 (1995)
6. K.P. Yuen, M.F. Law, K.W. Yu, Ping Sheng, Phys. Rev. E **56**, R1322 (1997)
7. L. Gao, K.W. Yu, Z.Y. Li, Bambi Hu, Phys. Rev. E **64**, 036615 (2001)
8. See, for example, the articles in *Proceedings of the First International Symposium on Functionally Graded Materials*, edited by M. Yamanouchi, M. Koizumi, T. Hirai, I. Shioda (Sendi, Japan, 1990)
9. A.M. Freyria, E. Chignier, J. Guidollet, P. Louisot, Biomaterials **12**, 111 (1991)
10. H. Karacali, S.M. Risser, K.F. Ferris, Phys. Rev. E **56**, 4286 (1997)
11. L. Gao, J.P. Huang, K.W. Yu, Phys. Rev. B **69**, 075105 (2004), and references therein
12. J.P. Huang, K.W. Yu, Appl. Phys. Lett. **85**, 94 (2004)
13. S. Suresh, A. Mortensen, *Fundamentals of Functionally Graded Materials*, IOM Communications Ltd., The Institute of Materials, London, 1998
14. *Functionally Graded Materials: Design, Processing and Applications*, edited by Y. Miyamoto, W.A. Kaysser, B.H. Rabin, A. Kawasaki, R.G. Ford (Kluwer Acadamic Publishers, Norwell, MA, 1999)
15. P.M. Hui, X. Zhang, A.J. Markworth, D. Stroud, J. Mater. Sci. **34**, 5497 (1999)
16. C.D. Van Siclen, Physica A **322**, 5 (2003)
17. D.A.G. Bruggeman, Ann. Phys. (Leipzig) **24**, 636 (1935)
18. H.R. Ma, R.F. Xiao, P. Sheng, J. Opt. Soc. Am. B **15**, 1022 (1998)
19. Y.M. Wu, L. Gao, Z.Y. Li, Phys. Stat. Sol. (b) **220**, 997 (2000)
20. D.J. Bergman, Phys. Rep. **43**, 378 (1978)
21. G.W. Milton, Appl. Phys. Lett. **37**, 300 (1980)
22. R.J. Gehr, G.L. Fisher, R.W. Boyd, J.E. Sipe, Phys. Rev. A **53**, 2792 (1996)
23. K.P. Yuen, M.F. Law, K.W. Yu, Ping Sheng, Opt. Commun. **148**, 197 (1998)
24. J.P. Huang, L. Dong, K.W. Yu, Europhys. Lett. **67**, 854 (2004)
25. O. Levy, D.J. Bergman, D.G. Stroud, Phys. Rev. E **52**, 3184 (1995)